TTCI TECHNOLOGY DIGEST

May 2020 TD20-007

The work described was performed by Transportation Technology Center, Inc., a wholly owned subsidiary of the Association of American Railroads.

Evaluation of In-Motion ECHO-Rail RCD Measurement System

Anish Poudel, Ph.D. and Matthew Witte, Ph.D.

Key Findings:

- ECHO-Rail shaped sensor indicated consistent defect detection and RCD measurement for speeds up to 20 mph.
- There was a small reduction in defect severity sensitivity of about 0.2 mm (0.008 inch) over the tested speed range from the walking speed. This was mainly attributed to reduced scan resolution as a result of increased sample spacing.
- Increased sample spacing (4 mm – 25 mm) may limit the ability to detect and measure isolated defects accurately. Smaller sample spacing is feasible at higher speeds with changes to the ECHO-Rail hardware.
- ECHO-Rail measurements at speed up to 20 mph agreed with prior experience at walking speed indicating that RCD tends to occur over relatively long intervals, often several yards. While the severity degree changes over that length, the rate of change appears to be somewhat gradual.

Transportation Technology Center, Inc. (TTCI) has continued working with Athena Industrial Services, Ltd. of Calgary, Canada, to bring forward ECHO-Rail, a prototype field-deployable hi-rail-mounted inspection system for characterizing rolling contact damage (RCD.) Prior issues of *Technology Digest* (TD)[1,2] described the capability of this technology to acquire crack and pit depth data from the running surface at walking speeds. This TD discusses the research and development of a hi-rail-based, full-scale prototype ECHO-Rail inspection system for RCD characterization.

In the previous work, the ECHO-Rail sensor was tested at walking speed on the Rail Defect Test Facility (RDTF) at the Transportation Technology Center (TTC), Pueblo CO. In this work, the sensor was mounted on the carriage of a hi-rail inspection vehicle and the testing was conducted on the High Tonnage Loop (HTL) at TTC. Athena made software modifications to accommodate the increased data rate and also updated graphic software to present the information in real time.

Inspection vehicle and carriage stability is an important factor that governs the higher test speeds. ECHO-Rail sensor has capabilities beyond 20 mph, but limitations of TTCI's hi-rail rail flaw inspection vehicle and carriage limited testing to a maximum speed of 20 mph.

BACKGROUND

Several research and test programs are currently being conducted to understand the root cause of RCD and to further improve wheel and rail life.[3] Previously published TDs provide a brief background on the measurement of RCD.[4,5] Management of RCD requires reliable, effective, and efficient non-destructive evaluation (NDE) technologies for detecting and characterizing surface flaws. Alternative NDE technologies that can perform accurate and efficient assessment of rail surface cracking while remaining insensitive to flaking and spalling are sought. The ideal NDE technology for RCD characterization would be non-contact, real-time, and in-motion capable.

ELECTROMAGNETIC FIELD IMAGING (EMFI) TECHNOLOGY

EMFI is a non-contact, electromagnetic NDE method that uses focusing elements to create focused electromagnetic field (EMF) and antennas to monitor EMF shape changes near the surface of a conducting material. Background on the fundamental principle of EMFI technology has been discussed in prior TDs.[1, 2]

EMFI technology is distinct from other available electromagnetic NDE technologies such as eddy current, Alternating Field Current Measurement (ACFM), or Magnetic Flux Leakage (MFL). Unlike conventional eddy current systems which measure amplitude and phase of the induced eddy current to derive measurement results, the amplitude and phase of the eddy current are not directly relevant in EMFI measurements. What is important in the EMFI approach is the bucking magnetic field (BMF) produced by the eddy current itself. The eddy current induced in the target material generates its own magnetic field that is in direct opposition to the EMF from the focusing element. This BMF "pushes" back on the EMF from the focusing element and causes the focused field shape to distort. As the local density of the BMF varies around the periphery of the sensor, so does the degree of shape distortion of the magnetic field from the focusing element. The antenna coils have a shape that is designed to directly measure the degree of electromagnetic field shape distortion.

Figure 1 shows the EMF states for different cases with and without the presence of flaws in the material. As shown: 1) null state; 2) sensor approaching transverse defect, amplitude (A) and phase (Φ) values shift toward positive; 3) sensor approaching longitudinal defects, (A) and (Φ) values shift toward negative, and; 4) sensor approaches shelling/spalling, (A) values shift towards positive and (Φ) values of EMF shift toward negative.

Figure 1 shows the EMF states for different cases with and without the presence of flaws in the material. The antenna coils produce an output voltage that is a proportional deviation of the mean magnetic field from a zero position; i.e., the neutral point. These signals, generated by the antenna coils, are then processed through a sequence of proprietary algorithms that allow crack direction and depth plus local changes in lift-off (corrosion, spalling, flaking) to be measured separately.

ECHO-RAIL HI-RAIL PROTOTYPE SYSTEM

An adapter was built to allow the ECHO-Rail sensor that was used previously on a walking stick to be mounted on the carriage of TTCI's hi-rail inspection truck. Figure 2 shows the adapter-sensor assembly and the inspection carriage.

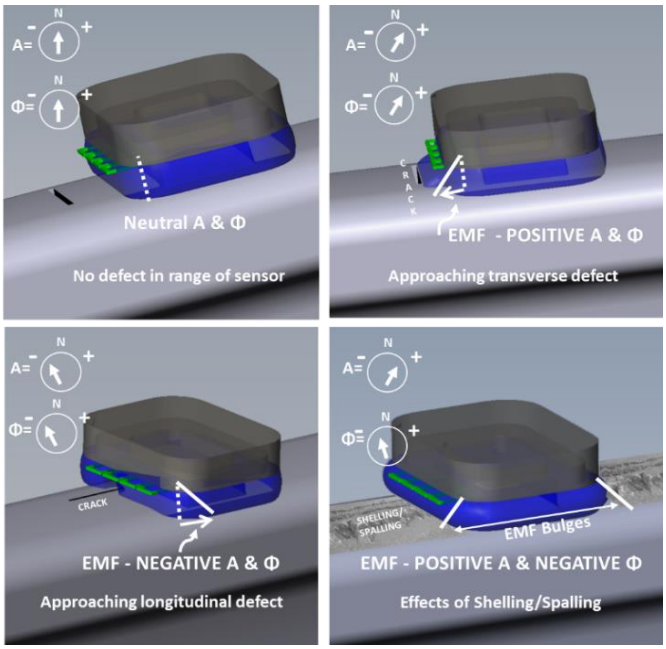

Figure 1. EMF shape for different defect types

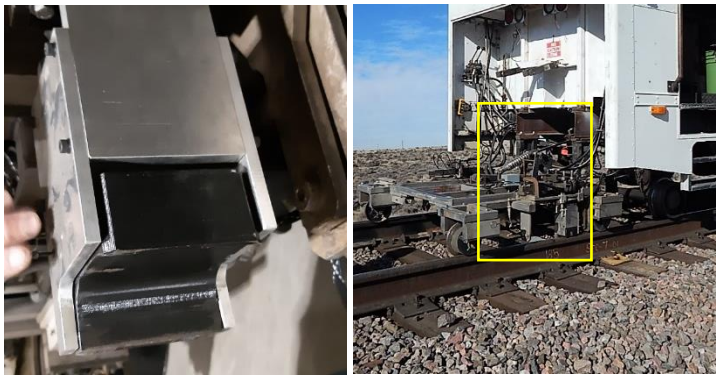

a. b.

Figure 2. Sensor mount and the carriage of the rail-inspection truck. (a) ECHO-Rail sensor mounted in the adapter; (b) controller and battery mounted in the carriage

ECHO-RAIL TESTING

Two areas of the HTL were chosen for repeatability tests, Section 3 (Tie No. 300-800) and Section 7 (Tie No. 0-240). In preparation for test, the sensor was aligned relative to the railhead. The stand-off distance from the face of the sensor module to the gage face was maintained to about 9.5 mm, and about 12 mm from the running surface of the rail. This testing

involved a series of runs over the specified rail sections at speeds of approximately 3, 6, 15, and 20 mph. Two runs were taken at each speed over both inside and outside rail sections. The sampling frequency of the transceiver is constant, so sample spacing necessarily varies with speed. Table 1 lists the sample spacing for different speeds.

Table 1. Sample spacing for each of the test speeds

Speed	Sample Spacing	
3.0 mph	4.0 mm	0.16 in.
6.0 mph	8.0 mm	0.32 in.
15.0 mph	16.0 mm	0.64 in.
20.0 mph	25.0 mm	0.98 in.

HTL TESTING RESULTS

Repeatability testing requires starting each run from the same precise location. Inaccurate calibration of the encoder as well as the need to realign data from different runs, due to varying start points, caused a slight misalignment between the actual defect locations and the distance indicated in the graphic shown for various HTL sections below.

Section 3, High Rail Joint at 35 feet (10 m)

Figure 3 shows a typical ECHO-Rail defect severity measurement for the rail joint for different speeds. It is observed that the magnitude of the defect responses were consistent for all speeds. The onset of the initial defect response varies from 29.8 feet (9.1 m) for 20 mph to 32.1 feet (9.8 m) for the 6 mph run. This was due to the result of carriage instability as the rail joint was crossed. Significant jarring of the vehicle was noted as the vehicle crossed the joint.

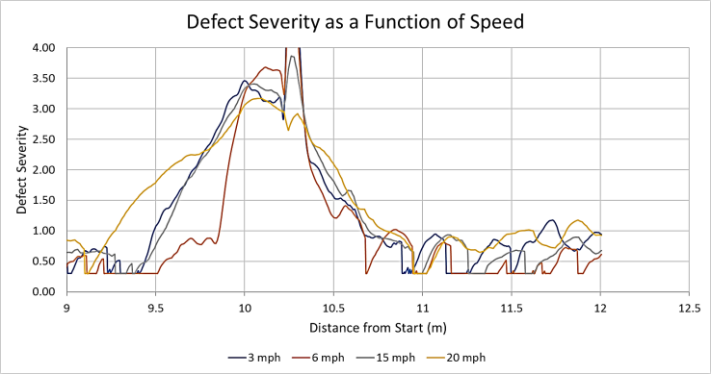

Figure 3. Echo-Rail defect severity measurement for the rail joint

Section 3, High Rail at 407 feet (124m)

Figure 4 show the ECHO-Rail defect severity measurements for the high rail in HTL Section 3, 407 feet from the starting point. Defect severity responses were generally consistent except for the 6-mph run, which shows a defect severity 0.5 less than the other runs. Inconsistent positioning of the sensor relative to the rail head may be responsible for this variance. Figure 5 shows the visual and liquid penetrant test result at this test location.

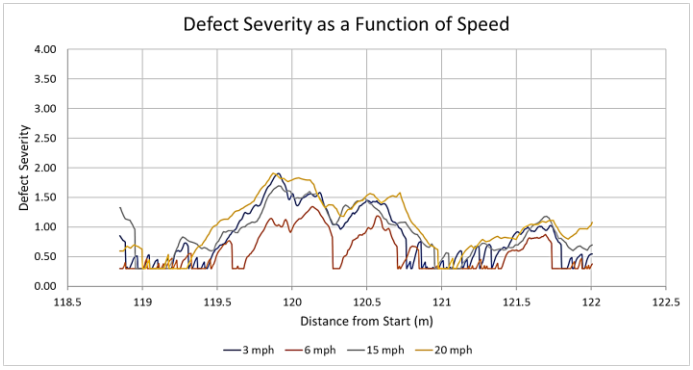

Figure 4. ECHO-Rail defect severity measurement for the high rail in HTL Section 3, 407 feet

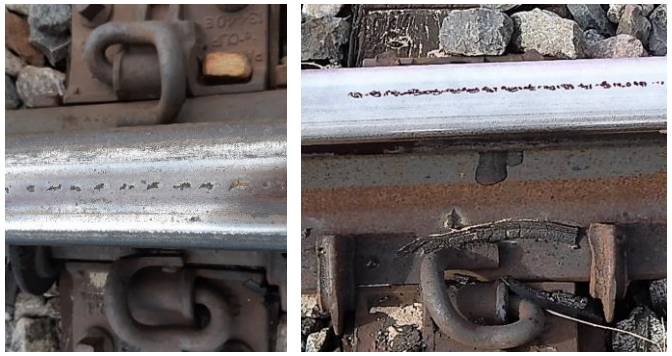

Figure 5. Visual and LPT test result for high rail, HTL Section 3, 407 feet

Section 3, Low Rail at 57 feet (17.4m)

Figure 6 shows the ECHO-Rail defect severity measurement for the low rail in HTL Section 3, 57 feet. RCD defect severity measurements were consistent for all speeds. Figure 7 shows the visual and liquid penetrant test result at that test location.

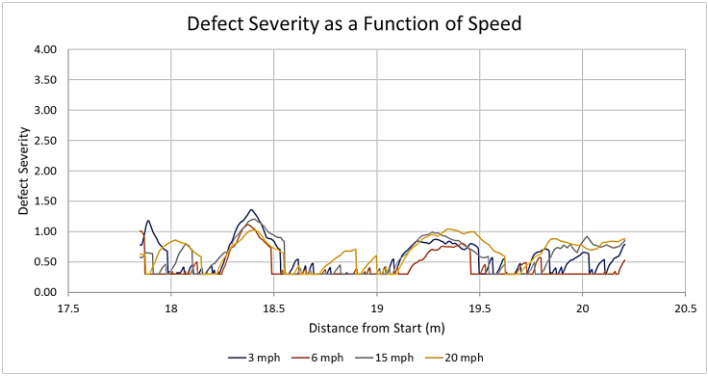

Figure 6. ECHO-Rail defect severity measurement for the low rail in HTL Section 3 at 57 feet location

Figure 7. Visual and LPT test result for the low rail in HTL Section 3 at 57 feet location

Section 7, High Rail Weld at 38 feet (12m)

Figure 8 shows the ECHO-Rail defect severity measurement for the high rail in HTL Section 7 at 38 feet. This location has a flash-butt weld and light RCD. The defect severity responses for the 3- and 6-mph tests and 15- and 20-mph tests were tightly grouped. The test vehicle was still accelerating for the higher speed tests of 15 mph and 20 mph. Significant jarring was present at this time, and the differences noted for the 15- and 20-mph runs may be related to the carriage instability. Results also indicate a jump in the defect severity value at the weld location. Dye penetrant and hand-UT analysis of this weld showed no defect present. Subsequent review suggested that the indication is primarily a function of the material property change associated with the weld. Further work will be required to optimize the analysis algorithm to compensate for the material change properties and process only the defect characteristics within the weld signature. Figure 9 shows the visual and liquid penetrant test result.

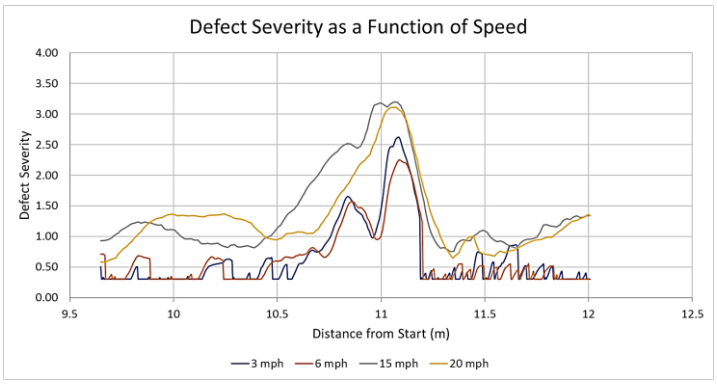

Figure 8. Echo-Rail defect severity measurement for the high rail in HTL Section 7 at 38 feet location

Figure 9. Visual and PT result for the high rail in HTL Section 7, 38 feet

CONCLUSIONS

Results from the evaluation of a hi-rail-mounted prototype ECHO-Rail inspection system indicate a high percentage of defect detection and severity consistent for speeds up to 20 mph. Carriage stability is an important factor that governs the higher test speeds. A speed of 20 mph does not indicate the upper limit of the ECHO-Rail sensor, but rather a limitation of TTCI's hi-rail inspection vehicle. Further improvements in processing algorithms will improve data at higher scan speeds. Additional high-speed tests need to be conducted in the future to determine a practical upper speed limit on the defect detection capabilities for RCD characterization.

References

1. Witte, M. and Poudel, A., May 2020, "Evaluation of ECHO-Rail Runner Scanning System for RCD Measurements," *Technology Digest* TD20-006, AAR/TTCI, Pueblo, CO.
2. Witte, M. and Poudel, A., July 2018, "Measuring Rolling Contact Damage in Rails Using EMFI," *Technology Digest* TD18-016, AAR/TTCI, Pueblo, CO.
3. Joy, R. and Tournay, H., 2011, "Rolling Contact Fatigue Workshop," DOT/FRA/ORD-12/08, Federal Railroad Administration, Washington, DC.
4. Witte, M., Poudel, A., and Fry, G., February 2018, "Rolling Contact Fatigue Measurement Using EMATs," *Technology Digest* TD18-004 AAR/TTCI, Pueblo, CO.
5. Baillargeon, J.P., and Tournay, H.M., May 2014, "Measurements Required to Manage Rolling Contact Fatigue," *Technology Digest* TD14-008, TTCI/AAR, Pueblo, CO.

For comments or questions about this publication, contact Anish_Poudel@aar.com